ASTFE
American Society
of Thermal and Fluids Engineers

5th Thermal and Fluids Engineering Conference (TFEC)
April 5–8, 2020
New Orleans, LA, USA

TFEC-2020-31962

POTENTIAL OF USING GRADED POROUS STAINLESS STEEL SUPPORT STRUCTURES TO IMPROVE ENERGY EFFICIENCY OF HYDROGEN SEPARATION IN STEAM REFORMING PROCESS

Davis S. Chamorro[1], Brian M. Fronk[1*]
[1]School of Mechanical, Industrial and Manufacturing Engineering
Oregon State University
Corvallis, OR 97331, USA

ABSTRACT

This study investigates the potential of using graded porous stainless steel (PSS) support structures to reduce the cost and size of membrane hydrogen separation units and maximize hydrogen production from steam reforming processes. Palladium (Pd) alloy composite membranes offer potential to reduce costs associated with distributed steam reforming by producing nearly pure hydrogen more efficiently and compactly than conventional separation methods. Typical membrane separator units consist of a thin Pd layer deposited on a PSS support structure. Due to the high cost of palladium, it is desired to minimize the amount used while also ensuring membrane reliability. The thickness of the deposited layer is largely determined by pore sizes on the surface of the support and can vary from 2 to 20 μm. Typical PSS support configuration includes a fine (1-10 μm pore radius) layer and one or two coarse (>10 μm) layers fabricated with selective laser sintering. Recent advances in additive manufacturing methods offer the potential to produce lower-cost PSS supports in which more finely graded pore size distributions can be produced. An analytical mass transfer model is developed to assess the impact of these different geometries on membrane unit performance for representative operating conditions. Preliminary results suggest improvements to the support geometry may increase hydrogen recovery by up to 20% for a given surface area.

KEY WORDS: hydrogen, membrane, Pd, PSS, steam reforming

1. INTRODUCTION

Increasing hydrogen demand has driven the need to improve its production and distribution methods. Of particular interest is the natural gas reforming process, which currently accounts for 48% of hydrogen production in the United States [1]. Existing natural gas delivery infrastructure and challenges associated with hydrogen delivery suggest distributed (~1,500 kg/day) natural gas reforming may be the most effective production method for the transition into a hydrogen economy. One challenge hindering the use of distributed steam reforming is high hydrogen cost compared to central production plants (~750,000 kg/day), which benefit from economy of scale [2-4]. Improved hydrogen purification methods at the back end of the reforming process that scale to expected distributed production levels may curtail this disparity.

The most common method of hydrogen purification is pressure swing adsorption (PSA), which uses multiple columns packed with adsorbent beds that remove hydrogen from the syngas stream through a series of drastic pressure changes [5]. Although very successful for central production, vibration sensitivity and cyclical operation make PSA undesireable for small scale production [5]. Highly selective Pd alloy membranes address these issues while producing nearly pure (99.99%+) hydrogen. Pd alloy membranes usually take the form of a thin layer of PdAg alloy deposited on a porous support structure in a countercurrent shell-and-tube form. The

*Corresponding Author: brian.fronk@oregonstate.edu

hydrogen-rich syngas flows on the shell side, with pure hydrogen permeating through the selective layer and out in the sweep gas, as seen in Figure 1.

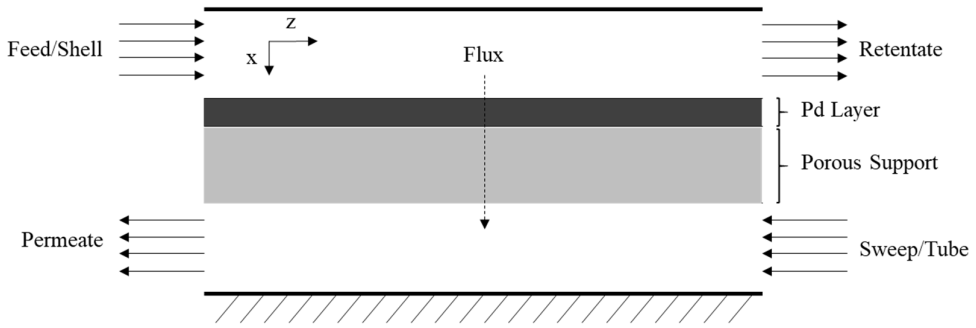

Fig. 1 A cross section of the membrane unit.

The porous structure provides mechanical support to the Pd layer as pressure differences between the feed and sweep can be up to 2 MPa [6,7]. These supports can be made from sintered stainless steel, porous ceramics, or glass. Sintered stainless steel is the most widely used option due to its ease of manufacturing, high mechanical durability, and similar thermal expansion coefficient to Pd, all of which are important for higher volume production [8,9]. Presently, porous stainless steel (PSS) supports are made using selective laser sintering (SLS) which uses a laser to sinter powdered stainless steel into a solid porous structure. Varying laser power and scan speed controls how particles sinter together and subsequently the porous structure properties (pore size, porosity, tortuosity) [10,11].

Prior research has shown that as surface pore size decreases, the required Pd thickness to avoid pinhole development also decreases [8]. A generally accepted rule of thumb is that the Pd layer thickness must be three times the diameter of the largest surface pore [8,9]. Current technology allows for PSS pore sizes as low as 0.1 μm; however, manufacturing costs have driven prior investigations to use supports with no more than three PSS layers (a very fine (0.1-1 μm) surface layer and up to two rough (5-10 μm) base layers), or ceramic supports that have smaller pore sizes but do not possess vital characteristics of PSS mentioned prior [12]. The growing use of additive manufacturing (AM) and subsequent improvement in technology may provide opportunity for supports with graded pore size distributions [13]. Nearly all research in Pd membrane based hydrogen separation has focused on the characteristics and transport through the membrane itself. However, the porous support structure is a significant resistance that cannot be neglected. Furthermore, the PSS represents an important cost driver, as the geometry and transport characteristics drive the Pd layer thickness. Thus, this study uses an analytical transport model to assess the influence of different PSS geometries possible through present SLS and future AM manufacturing methods on Pd membrane unit performance.

2. TRANSPORT MODEL DEVELOPMENT

Concentration-driven hydrogen transport through Pd alloy membranes follows a series resistance mechanism which includes bulk flow resistance, Pd layer resistance, and porous support resistance. Additional mass transfer resistance can be present on the sweep side and in the porous support depending on sweep conditions [14-16]. For this study it is assumed that the sweep side will be operating under vacuum with negligible resistance, as would be expected for conditions in which almost pure hydrogen is required [15].

2.1 Feed mass transfer

Hydrogen transport through the feed can be described using the Stefan-Maxwell equation assuming unimolecular flux as done by Hou & Hughes [17]:

$$N_{H_2} = \frac{\frac{k_H (P_{Hs} - P_{H1})}{RT}}{1 - \left[\frac{0.5 (P_{Hs} + P_{H1})}{P_T}\right]} \quad (1)$$

Here, P_{Hs} is the hydrogen partial pressure in the shell, P_{Hl} is at the Pd surface and P_T is the total shell pressure. The convective mass transfer coefficient, k_H, is approximated using a convective mass transfer correlation as described by Coulson et al. [18] for laminar flow and Welty et al. [19] for turbulent flow. For transport along the length of the membrane, z, a differential mass balance is performed over dz length.

2.2 Pd membrane mass transfer

Transport through the Pd layer can be modeled using a solution-diffusion mechanism as approximated by Sievert's Law:

$$N_{H_2} = Q \left(P^n_{H_2,high} - P^n_{H_2,low}\right) \quad (2)$$

Where Q is a permeance coefficient that takes on an Arrhenius form which depends mainly on temperature and Pd thickness, L, as described by Boon et al. [6].

When mass transfer through the Pd alloy layer is rate limiting, n=0.5 and Sievert's Law is obeyed. Deviations from n=0.5 suggest other steps are controlling hydrogen permeation, such as external mass transfer [5,17,20,21]. This study assumes transport through the Pd alloy layer is rate limiting and mass transfer inhibition effects such as polarization and CO/H_2O surface adsorption are negligible, based on the operating temperature, feed composition, and Pd thickness [1,6,17,22-27].

2.3 Porous support mass transfer

Transport through the porous support depends largely on the average pore size and kinetic energy of the transporting species. The Knudsen number, Kn, relates these parameters to determine the relative contribution of viscous flow and Knudsen diffusion [17,28]. For conditions and geometries common to Pd membrane operation, transport through the porous support is a combination of both viscous and Knudsen diffusion such that

$$N_{H_2} = \frac{2}{3}\frac{\varepsilon r}{\tau l}\left(\frac{8}{\pi RTM}\right)^{0.5} \Delta P + \frac{\varepsilon}{16\tau\eta}\frac{r^2}{RTl}\Delta P^2 \quad (3)$$

Where ε is porosity, r is the average pore radius, τ is the tortuosity, l is the support thickness, η is the hydrogen viscosity, and M is the molecular weight of hydrogen.

The support is divided into multiple layers – each of which uses Eq. 3 to predict the flux through the different layers. Figure 2 shows the geometry of the module used in this study.

Conservation of mass requires that the flux at each step of hydrogen permeation must be equal. Using *Engineering Equation Solver* [29], the system of equations can be solved. Numerical values used in Eq. 1, 2, & 3 are tabulated in Table 1. Pore sizes were chosen based on capabilities of PSS support manufacturers [12].

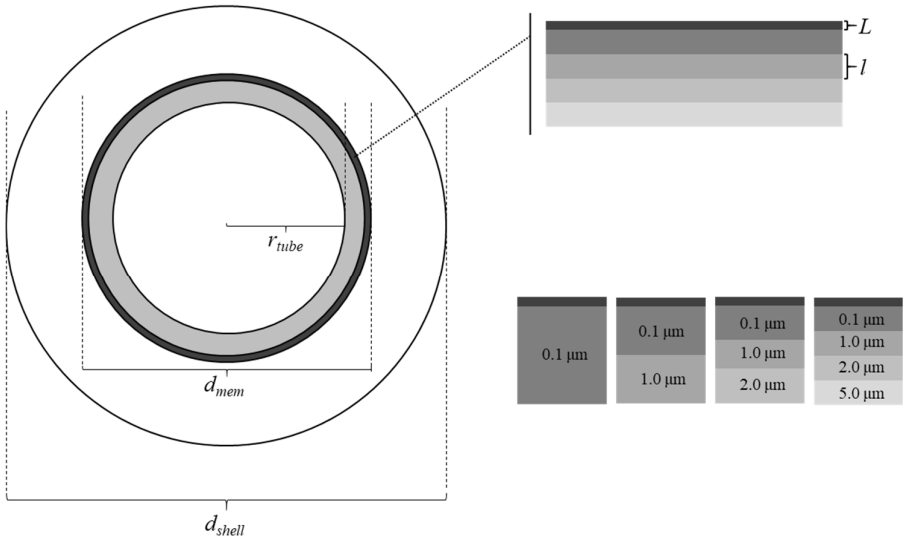

Fig. 2 Module geometry used for distributed production-scale simulations

Table 1 Numerical values used in flux Eq. 1, 2, & 3 for this study.

Variable	Value	Units	Variable	Value	Units
k_H	0.04	m s^{-1}	r	0.05-2.5	µm
Q	0.0003	mol m^{-2} $Pa^{-0.5}$ s^{-1}	η	2 x 10^{-5}	Pa s
L	5	µm	τ	1.25	-
n	0.5	-	l	0.75	mm
ε	0.5	-	M	2.2	kg $kmol^{-1}$

3. RESULTS AND DISCUSSION

3.1 Model Results

Model Validation. The model was validated using experimental results from Boon et al. [14] for a hydrogen-nitrogen feed. The membrane module was tested at 400 °C with a 55 mole% hydrogen feed at a total pressure of 3 MPa and varying sweep pressure with and without nitrogen as a sweep gas. The study used a ceramic support structure composed of a thin top layer with an average pore size of 80 nm on top of a coarse layer with an average pore size of 1.7 µm. Fig. 3 shows flux at three positions along the membrane for this work and values reported by Boon et al. [14].

The flux peaked at 0.65 mol m^{-2} s^{-1} at the inlet before dropping to below 0.1 mol m^{-2} s^{-1} near the outlet of the membrane. These fluxes are larger than those typically found when operating at conditions representative of larger scale hydrogen production and thus were only used to validate the present model.

Model Results. Once the model was validated it was used to investigate the effects of support pore size and distribution on a distributed production-scale process. As mentioned prior, the support often presents a significant mass transfer resistance and heavily influences the size and performance of the Pd layer [7,8]. To assess these impacts, four different support structure compositions were considered, ranging from uniform porosity of 0.1 µm

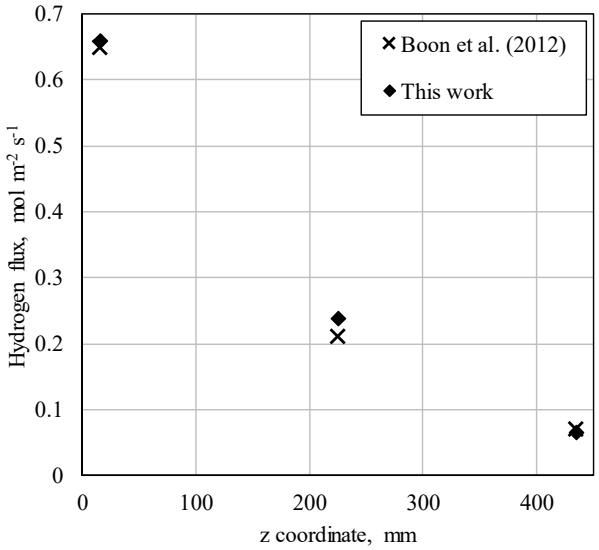

Fig. 3 Comparison of flux at different axial positions

to a graded porosity from 0.1 to 5.0 μm in four layers, as shown in Figure 2. These simulations were run at conditions representative of distributed production, assuming a hydrogen yield of 1,500 kg/day, as mentioned prior. This corresponds to a total membrane feed flowrate of 450 m^3 hr^{-1}. Membrane geometry and operating conditions are tabulated in Table 2. For the purpose of this study, a single tube design was modeled; however, future studies will model the membrane module in a multitube configuration, as would be expected in actual use.

Table 2 Operating conditions and membrane geometry

Variable	Value	Units	Variable	Value	Units
T	350	°C	d_e	0.1	m
$P_{shell,0}$	0.5	MPa	z	0-70	m
d_{shell}	0.2	m	$y_{H2,0}$	0.67	-
d_{mem}	0.1	m	P_{tube}	0	MPa
r_{tube}	0.047	m	V	450	m^3 hr^{-1}

As expected, the model predicted the maximum flux at the membrane inlet for all PSS support configurations, where the concentration driving force is largest. Values ranged from 0.012 to 0.062 mol m^{-2} s^{-1} for the single and four-layer supports, respectively. Fig. 4 shows hydrogen recovery in the shell as a function of membrane length for each support geometry configuration. Near the middle of the membrane length, the support utilizing four pore sizes results in as much as 20% more recovery than that of the single layer support. Additionally, the recovery is improved by slightly over 10% along the entire membrane.

Fig. 5 shows the reduction in membrane surface area required for a given percent recovery for each layer addition. Surface area reduction peaks at low percent recovery for all three scenarios. Near 80-90% recovery, the required surface area is reduced by ~10% for the addition of one layer, ~15% for the addition of two layers, and nearly 20% for the addition of three layers. The question then arises of which layer has the greatest impact on the membrane performance. Fig. 6 shows hydrogen partial pressure at each permeation step from the feed bulk to the sweep-side of the support structure. It is evident that the first layer of the support structure is presenting the largest mass transfer resistance, resulting in a larger pressure drop than any other support layer. This suggests that the benefit of using a graded support structure arises from minimizing the thickness of the

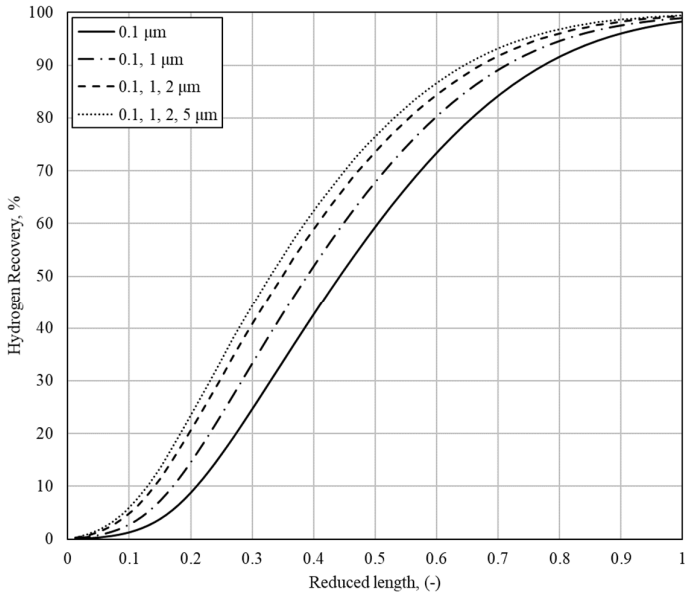

Fig. 4 Hydrogen recovery percent as a function of membrane length *L=80 m*

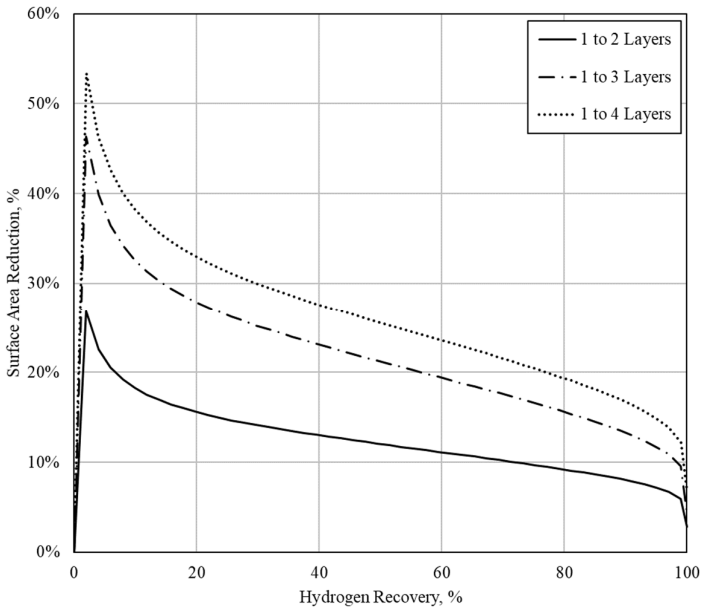

Fig. 5 Percent reduction in required surface area as a function of recovery for each coarse layer addition and subsequent layer thickness reduction.

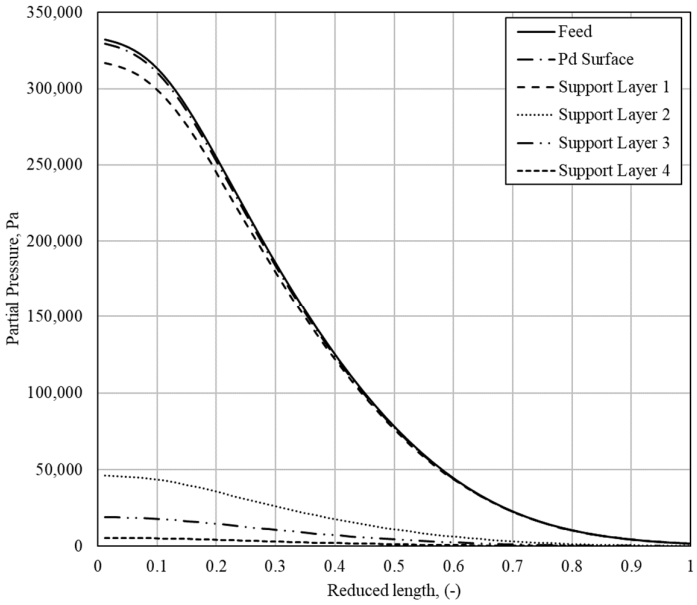

Fig. 6 Partial pressure of hydrogen at various points of permeation as a function of reduced length. *L=80 m*

fine surface layer. This is supported by Fig. 7 which shows the surface area required for a given percent recovery for both the four-layer support and a support which utilizes a similar thickness surface layer and three subsequent layers of larger pore size. Required surface area is identical for the two configurations, suggesting the surface layer – which is between 10 and 50 times finer than the subsequent layers – presents the largest mass transfer resistance. Practical implications of this result are discussed in the next section.

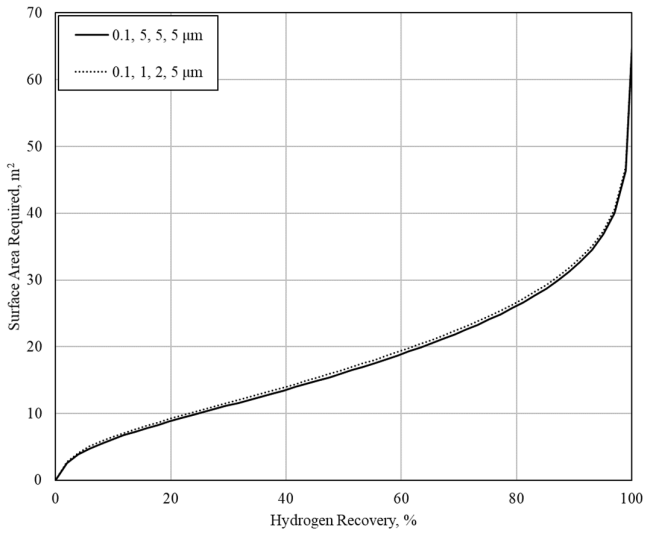

Fig. 7 Comparison of performance between the graded support and a support with equal top layer thickness and coarse bottom layers

4. CONCLUSIONS

An analytical model was constructed to predict mass transfer resistances and membrane performance for a composite Pd membrane utilizing a PSS support structure. The model was validated using experimental flux values reported in literature. The validated model was then used to investigate the use of different support pore sizes and distributions. Distributions in the support structure showed significant impacts on the overall membrane performance, with recovery varying by up to 20% for a given length. Studying the pressure drop at each permeation step revealed that the finest support layer contributes drastically more mass transfer resistance than the three following layers. This suggests that any changes made to the coarse support layers will present negligible changes in mass transfer resistance compared to those resulting from changing the finest layer. However, depositing a very fine layer on top of a very course layer may present manufacturing challenges. Additionally, a large pore size gradient between two layers may present issues associated with structural resistance to large pressure drops. This should be an area of future modelling and experimentation.

While this study assumes constant and uniform pore size on the surface, commercially available supports often show large variations in actual surface pore size [28]. Ensuring consistent pore size distribution would allow for better control over support layers and subsequent Pd thickness. Theoretically, depositing Pd onto a support with a 0.1 μm surface pores would only require a Pd thickness of 0.3 μm if applying the aforementioned rule of thumb [8,9]; however, current Pd deposition methods only allow for Pd layers of minimum 0.5-2 μm and Pd layers this thin present other mass transfer resistances [20,21,30-32]. Optimizing the membrane module design then becomes a tradeoff between minimizing Pd use and mitigating resulting mass transfer resistances caused by the ultra thin Pd.

Lastly, large membrane length scales predicted by this study suggest the use of multitube membranes may be required. Several studies have simulated small scale multitube designs for Pd membranes and have found improved mass transfer by the use of baffles within the module [23-25]. However, these studies were conducted using mass flows up to 100 times smaller than those used in this study and it is agreed upon that extensive research is necessary to better understand the scale-up behavior of the multitube module. [23-25]. To assess the impact of different scaled-up membrane module designs, a full steam reforming process simulation will be made using *Aspen HYSYS* [33]. Metrics such as energy input, hydrogen recovery, and membrane module cost will be evaluated.

REFERENCES

[1] DOE. (2013). Hydrogen, Fuel Cells and Infrastructure Technologies Program. *2002 Annual Progress Report*, *53*(9), 1689–1699. https://doi.org/10.1017/CBO9781107415324.004

[2] Thomas, C. (1998). Affordable hydrogen supply pathways for fuel cell vehicles. *International Journal of Hydrogen Energy*, *23*(6), 507–516. https://doi.org/10.1016/s0360-3199(97)00102-x

[3] Yang, C., & Ogden, J. M. (2005). Analyzing Natural Gas Based Hydrogen Infrastructure – Optimizing Transitions From Distributed To Centralized H2 Production. *National Hydrogen Association*, 20.

[4] Hecht, E. S., & Pratt, J. (2017). *Comparison of conventional vs. modular hydrogen refueling stations, and on-site production vs. delivery*. Retrieved from https://www.energy.gov/sites/prod/files/2017/03/f34/fcto-h2first-reference-station-phase2-2017.pdf

[5] Bhargav, A., Jackson, G. S., Ciora, R. J., & Liu, P. T. K. (2010). Model development and validation of hydrogen transport through supported palladium membranes. *Journal of Membrane Science*, *356*(1–2), 123–132. https://doi.org/10.1016/j.memsci.2010.03.041

[6] Boon, J., Pieterse, J. A. Z., van Berkel, F. P. F., van Delft, Y. C., & van Sint Annaland, M. (2015). Hydrogen permeation through palladium membranes and inhibition by carbon monoxide, carbon dioxide, and steam. *Journal of Membrane Science*, *496*, 344–358. https://doi.org/10.1016/j.memsci.2015.08.061

[7] Rothenberger, K. S., Cugini, A. V., Howard, B. H., Killmeyer, R. P., Ciocco, M. V., Morreale, B. D., … Ma, Y. H. (2004). High pressure hydrogen permeance of porous stainless steel coated with a thin palladium film via electroless plating. *Journal of Membrane Science*, *244*(1–2), 55–68. https://doi.org/10.1016/j.memsci.2004.06.036

[8] Mardilovich, I. P., Engwall, E., & Ma, Y. H. (2002). Dependence of hydrogen flux on the pore size and plating surface topology of asymmetric Pd-porous stainless steel membranes. *Desalination*, *144*(1–3), 85–89. https://doi.org/10.1016/S0011-9164(02)00293-X

[9] Hwang, K. R., Oh, D. K., Lee, S. W., Park, J. S., Song, M. H., & Rhee, W. H. (2017). Porous stainless steel support for hydrogen separation Pd membrane; fabrication by metal injection molding and simple surface modification. *International Journal of Hydrogen Energy*, *42*(21), 14583–14592. https://doi.org/10.1016/j.ijhydene.2017.04.032
[10] Furumoto, T., Koizumi, A., Alkahari, M. R., Anayama, R., Hosokawa, A., Tanaka, R., & Ueda, T. (2015). Permeability and strength of a porous metal structure fabricated by additive manufacturing. *Journal of Materials Processing Technology*, *219*, 10–16. https://doi.org/10.1016/j.jmatprotec.2014.11.043
[11] Shrestha, S., Starr, T., & Chou, K. (2019). *Porosity Analysis in Metal Additive Manufacturing by Micro-CT*. V002T02A059. https://doi.org/10.1115/imece2018-87897
[12] Palumbo, V., et al. Porous devices made by laser additive manufacturing. US 0239726, United States Patent and Trademark Office, 24 August 2017.
[13] Low, Z. X., Chua, Y. T., Ray, B. M., Mattia, D., Metcalfe, I. S., & Patterson, D. A. (2017). Perspective on 3D printing of separation membranes and comparison to related unconventional fabrication techniques. *Journal of Membrane Science*, *523*(October 2016), 596–613. https://doi.org/10.1016/j.memsci.2016.10.006
[14] Boon, J., Pieterse, J. A. Z., Dijkstra, J. W., & van Sint Annaland, M. (2012). Modelling and systematic experimental investigation of mass transfer in supported palladium-based membrane separators. *International Journal of Greenhouse Gas Control*, *11*(SUPPL), 122–129. https://doi.org/10.1016/j.ijggc.2012.09.014
[15] Nordio, M., Soresi, S., Manzolini, G., Melendez, J., Van Sint Annaland, M., Pacheco Tanaka, D. A., & Gallucci, F. (2019). Effect of sweep gas on hydrogen permeation of supported Pd membranes: Experimental and modeling. *International Journal of Hydrogen Energy*, *44*(8), 4228–4239. https://doi.org/10.1016/j.ijhydene.2018.12.137
[16] Barbieri, G. (2015). Encyclopedia of Membranes. *Encyclopedia of Membranes*, 1–2. https://doi.org/10.1007/978-3-642-40872-4
[17] Hou, K., & Hughes, R. (2003). Preparation of thin and highly stable Pd/Ag composite membranes and simulative analysis of transfer resistance for hydrogen separation. *Journal of Membrane Science*, *214*(1), 43–55. https://doi.org/10.1016/S0376-7388(02)00525-2
[18] Coulson, J. M., Richardson, J. F., Backhurst, J. R., & Harker, J. H. (1996). Fluid flow, heat transfer and mass transfer. In *Filtration & Separation* (Vol. 1). https://doi.org/10.1016/s0015-1882(96)90353-5
[19] Welty, J., Rorrer, G., & Foster, D. (2013). Fundamentals of Momentum, Heat, and Mass Transfer.
[20] Ward, T. L., & Dao, T. (1999). Model of hydrogen permeation behavior in palladium membranes. *Journal of Membrane Science*, *153*(2), 211–231. https://doi.org/10.1016/S0376-7388(98)00256-7
[21] Flanagan, T. B., & Wang, D. (2010). Exponents for the pressure dependence of hydrogen permeation through Pd and Pd-Ag alloy membranes. *Journal of Physical Chemistry C*, *114*(34), 14482–14488. https://doi.org/10.1021/jp101364j
[22] Li, A., Liang, W., & Hughes, R. (2000). The effect of carbon monoxide and steam on the hydrogen permeability of a Pd/stainless steel membrane. *Journal of Membrane Science*, *165*, 135–141.
[23] Castro-Dominguez, B., Mardilovich, I. P., Ma, R., Kazantzis, N. K., Dixon, A. G., & Ma, Y. H. (2017). Performance of a pilot-scale multitube membrane module under coal-derived syngas for hydrogen production and separation. *Journal of Membrane Science*, *523*(October 2016), 515–523. https://doi.org/10.1016/j.memsci.2016.10.024
[24] Coroneo, M., Montante, G., & Paglianti, A. (2010). Numerical and experimental fluid-dynamic analysis to improve the mass transfer performances of Pd-Ag membrane modules for hydrogen purification. *Industrial and Engineering Chemistry Research*, *49*(19), 9300–9309. https://doi.org/10.1021/ie100840z
[25] Ma, R., Castro-Dominguez, B., Dixon, A. G., & Ma, Y. H. (2018). Scalability of multitube membrane modules for hydrogen separation: Technical considerations, issues and solutions. *Journal of Membrane Science*, *564*(May), 887–896. https://doi.org/10.1016/j.memsci.2018.08.003
[26] Zhang, J., Liu, D., He, M., Xu, H., & Li, W. (2006). Experimental and simulation studies on concentration polarization in H 2 enrichment by highly permeable and selective Pd membranes. *Journal of Membrane Science*, *274*(1–2), 83–91. https://doi.org/10.1016/j.memsci.2005.07.047
[27] Chen, W. H., Syu, W. Z., & Hung, C. I. (2011). Numerical characterization on concentration polarization of hydrogen permeation in a Pd-based membrane tube. *International Journal of Hydrogen Energy*, *36*(22), 14734–14744. https://doi.org/10.1016/j.ijhydene.2011.08.043
[28] Nayebossadri, S., Fletcher, S., Speight, J. D., & Book, D. (2016). Hydrogen permeation through porous stainless steel for palladium-based composite porous membranes. *Journal of Membrane Science*, *515*, 22–28. https://doi.org/10.1016/j.memsci.2016.05.036
[29] EES: Engineering Equation Solver. F-Chart Software: Engineering Software. http://fchart.com/ees/.
[30] Nam, S. E., Lee, S. H., & Lee, K. H. (1999). Preparation of a palladium alloy composite membrane supported in a porous stainless steel by vacuum electrodeposition. *Journal of Membrane Science*, *153*(2), 163–173. https://doi.org/10.1016/S0376-7388(98)00262-2
[31] Xomeritakis, G., & Lin, Y. S. (1996). Fabrication of a thin palladium membrane supported in a porous ceramic substrate by chemical vapor deposition. *Journal of Membrane Science*, *120*(2), 261–272. https://doi.org/10.1016/0376-7388(96)00149-4
[32] Zhang, X., Xiong, G., & Yang, W. (2008). A modified electroless plating technique for thin dense palladium composite membranes with enhanced stability. *Journal of Membrane Science*, *314*(1–2), 226–237. https://doi.org/10.1016/j.memsci.2008.01.051
[33] Aspen HYSYS. Aspentech. https://aspentech/en/products/engineering/aspen-hysys